Astron. Astrophys. 356, 619–626 (2000)

ASTRONOMY AND ASTROPHYSICS

Hot star polarimetric variability and the nature of wind inhomogeneities

J.C. Brown[1,2], **R. Ignace**[1,4], **and J.P. Cassinelli**[1,3]

[1] Kelvin Bldg, Department of Physics and Astronomy, University of Glasgow, Glasgow, G12 8QQ, Scotland, UK
[2] Astronomical Institute "Anton Pannekoek", University of Amsterdam, Kruislaan 403, 1098 SJ Amsterdam, The Netherlands
[3] Sterling Hall, Department of Astronomy, University of Wisconsin, Madison, WI 53706-1582, USA
[4] Now at Physics and Astronomy, 203 Van Allen Hall, University of Iowa, Iowa City, IA 52245, USA

Received 10 May 1999 / Accepted 1 February 2000

Abstract. The problem is addressed of how much hot star polarisation variability can result from density redistribution processes within the wind as opposed to localised enhancement of stellar mass loss rate, such as ejections of wind inhomogeneities. For optically thin electron scattering, we present a theory for the relative polarisation arising from particle redistribution and consider several specific cases relevant to interpreting observations of wind variability. It is concluded that, allowing for partial cancellation of the contribution from compressed and evacuated regions, density redistribution internal to the wind can produce significant polarisation *but only* for processes that redistribute wind material over relatively large radial or angular scales. This conclusion favors extended spatial structures (e.g., from strong radiatively driven shocks) over localised condensations (e.g., from radiative instabilities).

Key words: polarization – stars: circumstellar matter – stars: early-type – stars: mass-loss – stars: variables: general

1. Introduction

Intrinsic polarisation from electron scattering polarisation in hot star winds requires an aspherical distribution of electron density. The quasi-steady, slowly varying, component of observed polarisation may be attributed to a mean rotationally symmetric wind structure, the magnitude of polarisation being determined by the product of envelope optical depth, a shape (asphericity) factor, and a viewing angle factor $\sin^2 i$ (Brown & McLean 1977). This description applies strictly in the single scattering limit, but is a reasonable approximation even for moderate optical depths (e.g., Daniel 1980). The more rapid variations (of order the wind flow time R_*/v_∞) are usually attributed to localised density enhancements, or "blobs", moving outward in the wind, these features also producing the photometric variability and transient narrow emission line features in Wolf-Rayet stars (e.g., Moffat et al. 1994; Robert 1994; Brown et al. 1995). Such blobs could originate in a number of ways, including local mass loss enhancements due to non-radial pulsations of a star near its Eddington limit and/or rotational limits (Langer 1998), or possibly localised aspherical features arising within the wind itself by processes such as radiative instability or radiatively driven shocks (Lucy 1982; Owocki & Rybicki 1984; Gayley & Owocki 1995). The amplitude of polarimetric variability can provide valuable information on the nature and origin of such blobs.

Brown et al. (1995), Richardson et al. (1996) and Li et al. (2000) have addressed the problem of the effect on polarimetric variability by the presence of substantial numbers of blobs, the random polarisations of which result in partial cancellation. For a large number N of blobs with a fixed *total* number of electrons in all N blobs, Brown et al. and Richardson et al. found that the polarisation declines as $1/\sqrt{N}$ owing to cancellation efffects. Here we address a different issue first raised by Brown (1994) concerning the polarimetric variability, namely the distinction between the effect of blobs created from local mass loss rate variations at the star and those arising from redistribution of the scattering electrons in the wind. The point is that density enhancements arising solely from the redistribution of electrons within an optically thin wind may produce little change in polarisation (tending to zero in some cases) *unless* the redistribution occurs over radial or angular scales that are substantial compared to (a) the radius of the star or (b) the angular extent over which the scattering angle influences the polarisation. The reason is that, in the optically thin limit, the contribution to the polarisation by the blob is proportional to the total number of scatterers, which does not vary upon redistribution, so that if the redistribution occurs over a small range of radius and angle, the polarisation is little changed. In this paper we quantify Brown's discussion for a number of simple cases relevant to stellar winds and discuss implications for shocks and other models of wind variability.

In Sect. 2, we specify our representation for wind clump density and derive the polarisation for several particular forms. In Sect. 3, the derived forms are used in considerations of redistribution of wind material from (a) conical slices that collapse to small dense bullets and (b) cones that collapse to conical caps. The former is a schematic representation for the case of a radiative instability and the latter for the case of a driven shock. A discussion of the results and applications is given in Sect. 4.

Send offprint requests to: J.C. Brown (john@astro.gla.ac.uk)

2. Polarisation of a parametric "blob" model

Polarisation resulting from electron scattering depends on moment integrals of the envelope electron density over the scattering volume (Brown & McLean 1977; Brown et al. 1978). Thus, for the present purpose of discussing the effect of polarisation of density changes on various scales, it will be sufficient to use a simple parametric model for the blob density. Analytic expressions for polarisation from Thomson scattering of stellar light are given by Brown & McLean (1977). These are based on the single scattering approximation, but work quite well at modest optical depths, especially for purposes of evaluating *relative* polarisations, rather than computing absolute values.

The Brown & McLean results apply to axisymmetric density structures only, but this will serve adequately to describe modifications of the polarisation resulting from changes in the wind electron density, either in the form of a plume or of a rotationally symmetric sector. In the former case, we take the plume to be axisymmetric about the central axis. We can also use this case to describe a localised "point" scattering region simply by giving the plume very small radial and angular extent. For the annular sector, the symmetry axis is that of the annulus. Brown & Mclean showed that the polarisation of *any* axisymmetric structure could be written as the product of an optical depth factor (scaling with $N_{\rm e}$ the total number of electrons and the inverse square of the system size), an asphericity shape factor, and a viewing inclination factor $\sin^2 i$. To the Brown & McLean expressions, we add the depolarisation correction factor derived by Cassinelli et al. (1987) and by Brown et al. (1989) for finite star size, although we do not account for envelope occultation by the stellar disk.

As illustrated in Fig. 1, our basic blob model is an axisymmetric density structure which is uniform over a range of colatitude ϑ, in the interval (μ_1, μ_2) with $\mu = \cos\vartheta$, and has an $n \sim r^{-2}$ radial variation of density in the range of radii (r_1, r_2). For such a blob, the electron number density is taken as $n_{\rm e} = n_0\, R^2/r^2$ for $n_0 = n_{\rm e}(R)$ a scale constant and R the stellar radius, hence the total number of electrons is

$$N_{\rm e} = \int n_{\rm e}\, dV = 2\pi\, n_0\, R^2\, (r_2 - r_1)(\mu_2 - \mu_1). \quad (1)$$

Using expressions from Brown & McLean (1977), the polarisation of the blob is given by

$$P = \frac{3}{16}\sigma_{\rm T} \sin^2 i \int_{r_1}^{r_2} \int_{\mu_1}^{\mu_2} n_{\rm e}(r) \sqrt{1 - \frac{R^2}{r^2}} (1 - 3\mu^2)\, dr\, d\mu. \quad (2)$$

where the square root factor accounts for the depolarisation effects of the finite stellar size (Cassinelli et al. 1987). Evaluating the radial and latitudinal integrals and eliminating n_0 in favor of $N_{\rm e}$, the resulting blob polarisation becomes

$$P = \frac{3}{32\pi} \frac{\sigma_{\rm T}\, N_{\rm e}\, \sin^2 i}{(r_2 - r_1)(\mu_2 - \mu_1)} \times \int_{r_1}^{r_2} \frac{1}{r^2} \sqrt{1 - \frac{R^2}{r^2}}\, dr \int_{\mu_1}^{\mu_2} (1 - 3\mu^2)\, d\mu. \quad (3)$$

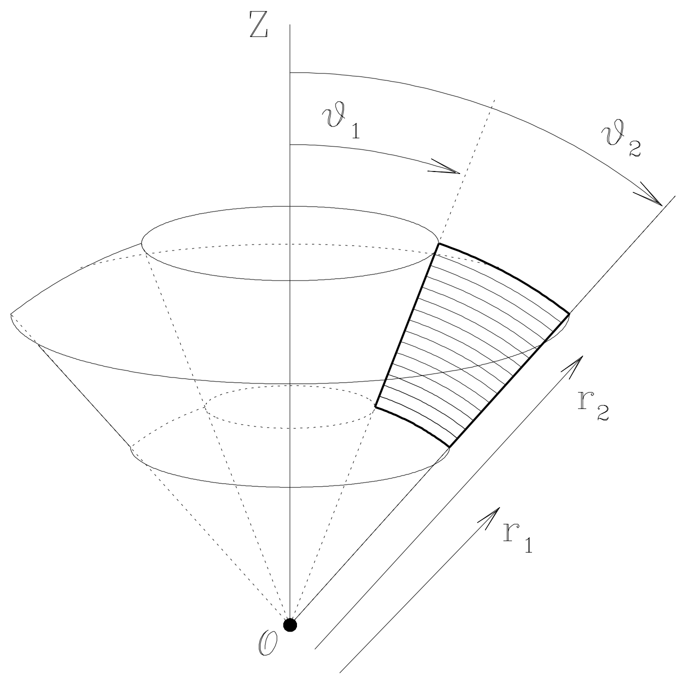

Fig. 1. The figure shows the geometry assumed throughout the paper. A conical region is defined to exist in the interval of angle from ϑ_1 to ϑ_2 and of radius from r_1 to r_2. The conical volume is assumed azimuthally symmetric about the central axis Z, and we further assume the density of electrons to diminish with distance as $1/r^2$. The cone is thus a volume of revolution formed by the wedge patch as shown.

Adopting as a constant scale parameter,

$$P_0 = \frac{3}{32\pi} \frac{\sigma_{\rm T}\, N_{\rm e}}{R^2} \sin^2 i, \quad (4)$$

and using a normalized radius $x = r/R$, we define the scaled polarisation to be

$$p = \frac{P}{P_0} \quad (5)$$

$$= [1 - (\mu_1^2 + \mu_1\mu_2 + \mu_2^2)] \left\{ \frac{\sin^{-1} 1/x_1 - \sin^{-1} 1/x_2}{2(x_2 - x_1)} + \frac{x_1^{-1}\sqrt{1 - 1/x_1^2} - x_2^{-1}\sqrt{1 - 1/x_2^2}}{2(x_2 - x_1)} \right\} \quad (6)$$

$$\equiv g(\mu_1, \mu_2)\, f(x_1, x_2), \quad (7)$$

The two functions g and f are conveniently defined to separate the dependence of the polarisation on angular extent and radial extent. The two functions are given by

$$g(\mu_1, \mu_2) = 1 - (\mu_1^2 + \mu_1\mu_2 + \mu_2^2) \quad (8)$$

and

$$f(x_1, x_2) = \frac{\sin^{-1} 1/x_1 - \sin^{-1} 1/x_2}{2(x_2 - x_1)} + \frac{x_1^{-1}\sqrt{1 - 1/x_1^2} - x_2^{-1}\sqrt{1 - 1/x_2^2}}{2(x_2 - x_1)}. \quad (9)$$

The advantage of the scaled polarisation p is that a prescribed number of scattering electrons is maintained for any redistribution in x and μ. Hence the nett relative change in the scaled polarisation arising from redistribution is neatly given by the difference in p for the two respective structures with the same N_e.

Here we derive expressions for the scaled polarisation from a number of specific simplified cases. These results are used in the following section to determine the scaled polarisation arising from redistribution of a fixed number of scatterers in geometries of interest to stellar winds. We consider the cases of scattering by a point blob, a conical cap, and a wedge sector (e.g., a disk):

(a) Localised point scattering.

Setting $\mu_1 = \mu_2 = 1$ and allowing $x_1 \to x_2 \to x_0$ in (2), the scaled polarisation from a point blob is

$$p_\mathrm{point} = -2\,\frac{1}{x_0^2}\sqrt{1-\frac{1}{x_0^2}}. \tag{10}$$

This has an extremum value $p_\mathrm{max} = -4/3\sqrt{3}\,(=-0.77)$ at $x_0 = \sqrt{3/2}\,(=1.22)$, which presents the maximum scaled polarisation resulting from any distribution of a prescribed number of electrons, thus providing a convenient benchmark used in subsequent discussion. The actual polarisation would be $P_\mathrm{max} = P_0\,p_\mathrm{max} = -0.77P_0$, hence P_0 is of the same order as $|P_\mathrm{max}|$. Note that we have adopted a convention for which a negative polarisation refers to a polarisation position angle perpendicular to the axis of symmetry; the position angle for positive polarisation is thus parallel to that axis.

(b) Scattering by a conical cap.

Here we consider the case of part of a conical plume with opening angle $\mu_1 = \cos\vartheta_1$ and $\mu_2 = 1$ to give

$$p_\mathrm{cone} = -\mu_1(1+\mu_1)\,f(x_1,x_2). \tag{11}$$

For a conical cap of small radial extent, such that $x_2 \to x_1 \to x_0$, the scaled polarisation reduces to

$$p_\mathrm{cone} = \frac{1}{2}\,\mu_1(1+\mu_1)\,p_\mathrm{point}. \tag{12}$$

This latter case is of interest as representing a radially narrow density enhancement such as produced by a shock.

(c) Scattering by a wedge sector.

Here we are seeking to describe the polarisation of an equatorial wedge sector of scatterers (as for example to approximate the density structure of a Wind Compressed Zone model from Ignace et al. 1996). We take $\mu_1 = -\mu_2$, so that the scatterers exist only for latitudes $-\mu_2 < \mu < \mu_2$, which gives

$$p_\mathrm{sec} = (1-\mu_2^2)\,f(x_1,x_2). \tag{13}$$

For a flat annular disk $(\mu_2 \to 0)$ of finite radial width, the scaled polarisation is

$$p_\mathrm{disk} = f(x_1,x_2), \tag{14}$$

whereas for a radially narrow annular rim with $x_2 \to x_1 \to x_0$, but μ_2 finite,

$$p_\mathrm{rim} = -\frac{1}{2}\,(1-\mu_2^2)\,p_\mathrm{point}. \tag{15}$$

Note that in contrast to the conical cap of case (b), the polarisations p_rim and p_point have opposite signs, as expected since the rim case is oriented symmetric to the equatorial plane, whereas the point case is taken to lie along the polar axis.

3. Polarisations arising from matter redistribution

As suggested in Sect. 1, some wind density blobs might arise by local enhancements of stellar mass loss through the photosphere. These represent an absolute deviation from spherical symmetry (or other smooth distributions, like an ellipsoid), in the sense that there is an increase in mass along some ray paths from the star without compensating decreases along other ray paths. On the other hand, some blobs may arise from density redistribution within the wind above the photosphere. For example, firstly, a small random density enhancement may increase radiative cooling, so reducing pressure, and precipitating radiatively unstable collapse of a wind region into a cooler denser "condensation" in the wind. Secondly, in contrast to this *intrinsically* unstable process, dense local structures in the wind may arise through the formation of shocks via the line-*driven* instability mechanism (Lucy 1982; Owocki & Rybicki 1984). The shocks then "sweep up" mass along a region of constant solid angle, or "cone", in the wind. This scenario for wind shocks is almost certainly occurring in hot star winds as evidenced by UV resonance line profile variability (Gathier et al. 1981; Lamers et al. 1982; Massa et al. 1995; Kaper et al. 1999) and the multi-million degree temperature X-ray emission (Cassinelli & Swank 1983; Kudritzki et al. 1996; Feldmeier et al. 1997).

For conservative redistribution, no new electrons are added to the wind and the polarisation resulting from the dense "blob" is partially offset by the negative polarisation of the evacuated region (i.e., the polarisation of the total wind volume without the dense blob). The extent of this cancellation, which we shall hereafter refer to as the "cavity effect", depends on the specific redistribution geometry, so we next consider several particular cases using results from the preceding section.

Bear in mind that it is the *change* in scaled polarisation, not the actual polarisation itself, that we will be computing. The initial geometry is assumed spherical, which yields zero net polarisation. After redistribution the nett scaled polarisation is the difference between that arising from the compressed region and that of the spherical wind minus the cavity. The polarisation[1] would then be the scaled polarisation p multiplied by the scale factor P_0 from Eq. (4).

[1] More generally, the polarisation is a proper Stokes vector sum of that from the redistributed volume and that from outwith the redis-

3.1. *Collapse of a conical volume to a point*

Consider the collapse of electrons in a conical element, as described by result (b) of Sect. 2, down to a point scattering region that lies within the element and on the cone's central axis. Outside this element, the wind remains unchanged. Note that use of the point blob as the geometry for redistributed wind material ensures that the scaled polarisation is maximized; any other redistribution geometry will produce smaller changes. The resulting nett scaled polarisation is

$$p = p_{\rm point} - p_{\rm cone} = \mu_1(1+\mu_1) f(x_1, x_2) - 2\frac{1}{x_0^2}\sqrt{1-\frac{1}{x_0^2}}, \quad (16)$$

where $x_1 \leq x_0 \leq x_2$.

Fig. 2 plots the value of p in such a scenario for different values of x_0 and μ_1. The value of x_1 is fixed at unity (i.e., the stellar surface), and the results for p are plotted against the ratio of x_0 for the collapsed point to x_2 for the outer boundary of the original conical volume. Solid curves are for $\mu_1 = 1$ (narrow polar plume), short dashed for $\mu_1 = 1/\sqrt{3}$ (the van Vleck angle), and long dashed for $\mu_1 = 0$ (hemisphere). The van Vleck (1925) angle of $54.°7$ corresponds to the latitude at which the nett polarisation of a circular ring undergoes a change of sign; rings at higher latitudes have a "polar-like" polarisation (negative in our convention) and rings at lower latitudes are "equator-like" (positive polarisation). Consequently, we use a value of μ_1 at the van Vleck angle as a canonical intermediate case between the extremes of a polar plume and hemisphere. The three curves beginning furthest left are for $x_2 = 10$, and the other three are for $x_2 = 3$. Note that because $x_1 = 1$, all of the curves pass through zero at least once, hence there exists a position interior to the conical volume where the collapse of all the electrons to a dense point *does not* produce *any* change in the polarisation. This is the essence of Brown's (1994) discussion.

3.2. *Radial compression of a conical volume*

The shocked regions in a stellar wind can be represented by a "driven wave" as discussed by Hundhausen (1985) and MacFarlane & Cassinelli (1989). The density enhancement associated with a shock "contact surface" in the wind could be near the forward facing shock where the driven wave overtakes the material ahead of it. Or, it could be near the rearward shock where faster wind from behind collides with the driven wave. Both compression situations are possible because the density rise occurs where the radiative cooling of post-shock material is most rapid. This is illustrated in Figs. 12.3 and 12.4 in Lamers & Cassinelli (1999). Feldmeier et al. (1997) suggest that the shock structure responsible for the X-ray emission from O stars is perhaps more like the forward facing kind of MacFarlane & Cassinelli (1989) rather than the rearward shock type of Owocki & Rybicki (1984). Here we treat both cases individually.

tributed volume, which may be of arbitrary shape and density distribution. The initially spherical case is especially interesting since the polarisation from redistribution within a part of the spherical envelope yields the same result as if the redistributed volume were in isolation.

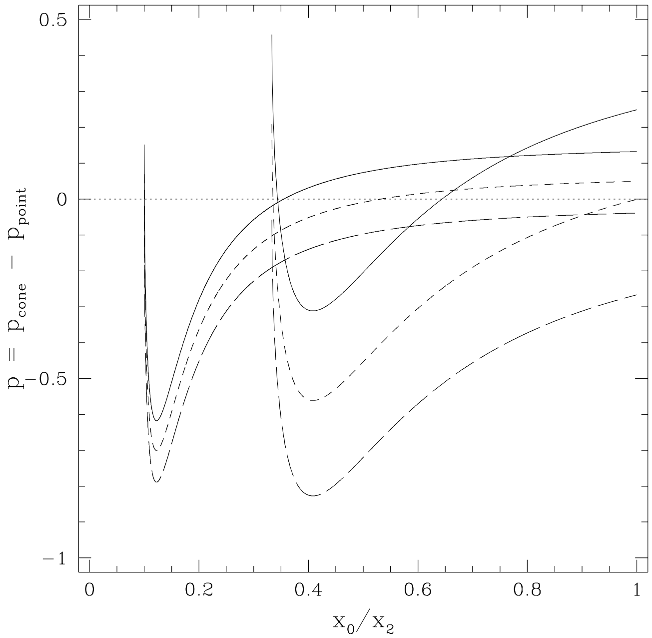

Fig. 2. The figure shows the scaled polarisation, $p = P/P_0$, for the case of a conical volume of scatterers that has collapsed to a point at x_0. The value of the initial inner radius $x_1 = 1$ is fixed in all cases, and x_0 is allowed to vary only betwen x_1 and x_2, thus p is plotted against the ratio x_0/x_2. Solid curves are for $\mu_1 = 1$, short dashed for $\mu_1 = 1/\sqrt{3}$ the van Vleck angle, and long dashed for $\mu_1 = 0$. The three curves extending leftmost are for $x_2 = 10$; the other three are for $x_2 = 3$.

For the evolution of a shock, the idea is that an instability results locally in cones of the wind, leading to an accumulation of mass into a cap geometry (either forward facing from overtaking upwind material or rearward facing from faster wind material that overtakes the shock). We assume the shock moves radially outward within the boundaries of the cone. Here we are mainly concerned to see how large the effect will be on polarisation of such sweeping of a fixed amount of material within the wind in a localised domain such as within a cone. We consider the case of a conical region of fixed opening angle. If we start with material in the interval (x_1, x_2) and drive it into the interval (x_1', x_2') included in (x_1, x_2), then the nett scaled polarisation that results is

$$p_{\rm shock} = -\mu_1(1+\mu_1)\,[f(x_1', x_2') - f(x_1, x_2)]. \quad (17)$$

3.2.1. Forward facing shock

We deal first with the case of a forward facing shock that we shall refer to as "snowploughing", for it sweeps up the preceding wind. The anticipated effect will be to drive most of the material to the outer boundary of the redistribution volume. To describe this, we define the radial width of the affected volume $L = x_2 - x_1$, the radial width of the redistributed volume $\Delta = x_2' - x_1'$, and set $x_2' = x_2$. The two functions of radius become

$$f(x_1, x_2) = \frac{1}{2L}\Big[\sin^{-1} 1/(x_2 - L) - \sin^{-1} 1/x_2$$

$$+ (x_2 - L)^{-1}\sqrt{1 - 1/(x_2 - L)^2} - x_2^{-1}\sqrt{1 - 1/x_2^2}\Big],$$

and

$$f(x_1', x_2') = \frac{1}{2\Delta}\Big[\sin^{-1} 1/(x_2 - \Delta) - \sin^{-1} 1/x_2 \quad (18)$$
$$+ (x_2 - \Delta)^{-1}\sqrt{1 - 1/(x_2 - \Delta)^2} - x_2^{-1}\sqrt{1 - 1/x_2^2}\Big].$$

Of course, the Eqs. (18) and (19) are only valid if $L \geq \Delta$.

In the limit of the shock region being relatively narrow, we can take $\Delta \ll 1$ leading to the simplification that

$$f(x_1', x_2') \approx \frac{1}{x_2^2}\sqrt{1 - \frac{1}{x_2^2}}. \quad (19)$$

In the context of a shock that forms just at the photosphere, we allow $x_1 \to 1$ hence $x_2 = 1 + L$, giving for the nett scaled polarisation

$$p_{\rm shock} = -\mu_1(1+\mu_1)\Big\{(1+L)^{-2}\sqrt{1 - 1/(1+L)^2}$$
$$- (2L)^{-1}\Big[\frac{\pi}{2} - \sin^{-1} 1/(1+L)$$
$$- (1+L)^{-1}\sqrt{1 - 1/(1+L)^2}\Big]\Big\}. \quad (20)$$

In the limit that $L \gg 1$, the nett change in scaled polarisation reduces to just

$$p_{\rm shock} = \mu_1(1+\mu_1)\,\frac{\pi}{4L}. \quad (21)$$

Note that in this expression, $p_{\rm shock}$ has the same sign as μ_1, meaning that it is the polarisation contribution of the evacuated region (i.e., of the wind with a cavity in it) and *not* of the dense snowploughed material that determines the polarisation position angle. Hence the position angle is parallel to the axis of the cone and not perpendicular to it, as one might expect from scattering by the dense shock. The fact that the cavity is of prime importance in determining the polarisation is a consequence of its being interior to the outward moving shock. If for example the mass concentration were instead inward at say $x_1' = x_1$, there would be a change of sign in the expression for $p_{\rm shock}$, and the mass concentration would then be of prime importance in fixing the polarisation.

Fig. 3 shows $p_{\rm shock}$ as plotted against $\log(1 + L)$ for four values of $\Delta = 0.0, 0.1, 0.3$, and 1.0. The scaled polarisation is normalized by the factor $\mu_1(1+\mu_1)$ that describes the opening angle of the cone. The value of $p_{\rm shock}$ is zero for $L = \Delta$ and has a L^{-1} tail at large L, as predicted in Eq. (21). The curves also show that $p_{\rm shock}$ can change sign as L changes. At large L, $p_{\rm shock}$ is positive indicating that the cavity is determining the nett scaled polarisation and position angle. However, at small L where the swept up cavity is small (on the order of Δ or smaller), $p_{\rm shock}$ is negative, and it is the dense material and not the cavity that is dominating the polarisation.

In the most favorable case, the fractional change in polarisation (i.e., $\Delta p/p = \Delta P/P$) does not much exceed 0.1 at best. Thus for example, if all the cone electrons alone could produce a maximum of say 1% polarisation when optimally distributed, then the biggest polarisation which could result in a spherical wind by forward shock concentration of the electrons within a cone would be 0.1%. The radial extent over which $p_{\rm shock}$ is at least half this value is from $x \approx 1$ to $x \approx 10$. The typical "flush time" R_*/v_∞ for hot early type stellar winds is a few hours, hence polarimetric variability from the formation of shocks will be around 5–10% over a period of around 1 day if the shock forms near the base of the wind.

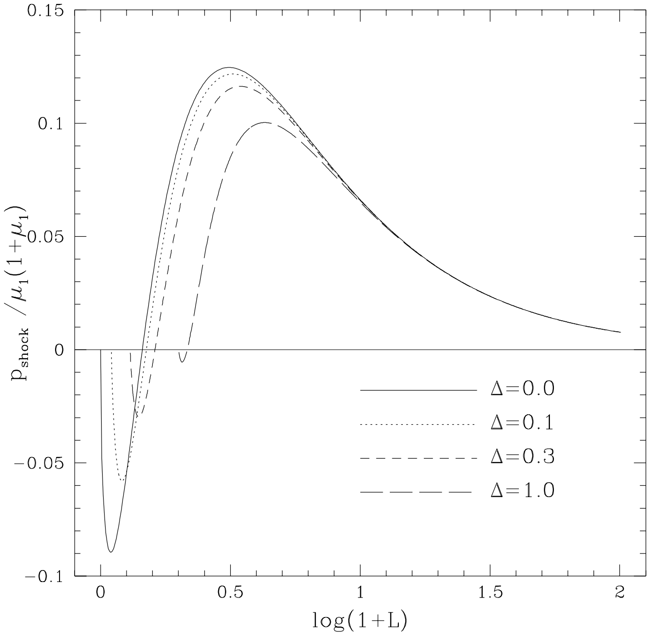

Fig. 3. The figure shows the scaled polarisation $p_{\rm shock}$ against $\log(1 + L)$ for the radial compression of a conical volume. This scenario is to represent the formation of a shock, with the dense swept up material at the outer boundary of the cone with radial width $\Delta = 0.0, 0.1, 0.3$, or 1.0 as indicated, and the trailing region approximated as a vacuum cavity of extent $L - \Delta$. Note that $p_{\rm shock}$ is normalized by $\mu_1(1+\mu_1)$, so that the plotted curve does not depend on the opening angle of the cone. (Further note that the inner radius of the conical volume x_1 is taken as unity for the case shown.)

3.2.2. Rearward facing shock

Now we consider the opposite example of a rearward facing shock. In the case of the forward facing shock, a cavity was cleared out so that material was driven into a conical cap at the outward face of the cone. The cavity was allowed to stretch back to the star, which is not realistic since wind material should always be flowing out of the star and into the cone, however it allows maximisation of the scaled polarisation change. In the rearward shock case, we consider wind material to accumulate in a conical cap at the inward face of the cavity. Here we allow this dense cap to move outward instead of keeping it fixed at the wind base.

For the scaled polarisation, we note that the result derives essentially from the previous expressions (17)–(19), but with a slight modification. We can still use the definitions of L and Δ, but now require that $x_1' = x_1$ instead of $x_2' = x_2$. The

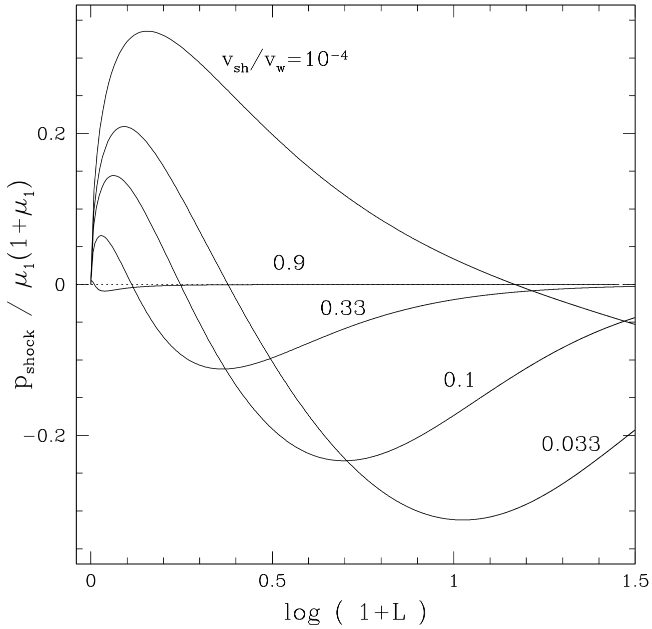

Fig. 4. The figure shows the scaled polarisation $p_{\rm shock}$ normalized by $\mu_1(1+\mu_1)$ as plotted against $\log(1+L)$ for the radial compression of a conical volume, in this case a rearward facing shock. Here the dense material results from wind that catches up to a slower outward moving shock. Both the wind and the shock are assumed to move at constant speed. Different curves are for different ratios of shock to wind speed, $v_{\rm sh}/v_{\rm w}$, as labeled. The positive value of the $p_{\rm shock}$ indicates that the cavity is of prime importance, and not the dense shock, in determining how the polarisation evolves as the structure propagates through the flow. Negative values indicate that the dense shock is predominant over the cavity.

expressions become

$$f(x_1,x_2) = \frac{1}{2L}\Big[\sin^{-1} 1/(x_2-L) - \sin^{-1} 1/x_2 + (x_2-L)^{-1}\sqrt{1-1/(x_2-L)^2} - x_2^{-1}\sqrt{1-1/x_2^2}\Big], \quad (22)$$

and

$$f(x_1',x_2') = \frac{1}{2\Delta}\Big[\sin^{-1} 1/(x_2-L) - \sin^{-1} 1/x_2' + (x_2-L)^{-1}\sqrt{1-1/(x_2-L)^2} - x_2'^{-1}\sqrt{1-1/x_2'^2}\Big]. \quad (23)$$

In the limit of the shock region being relatively narrow, we again take $\Delta \ll 1$ leading to the simplification that

$$f(x_1',x_2') \approx \frac{1}{x_1^2}\sqrt{1-\frac{1}{x_1^2}}. \quad (24)$$

If the shock begins just at the photosphere, we allow $x_1 = x_1' = x_2 = x_2'$ at time $t=0$. If we knew how x_1 and x_2 evolved with time, we could simply use Eqs. (23) and (24) with (17) to determine the time evolution of $p_{\rm shock}$. However, existing observations do not provide such knowledge at this time, and best estimates would have to come from complicated time-dependent theoretical calculations. So as an illustrative example, we choose to model the shock as follows, letting

$$x_1 = 1 + t/\tau_{\rm sh}, \quad (25)$$

$$x_2 = 1 + t/\tau_{\rm w}, \quad (26)$$

$$x_2 - x_1 = L = \left(\frac{\tau_{\rm sh}-\tau_{\rm w}}{\tau_{\rm w}\,\tau_{\rm sh}}\right) t, \quad (27)$$

where $\tau_{\rm sh} = R_*/v_{\rm sh}$ and $\tau_{\rm w} = R_*/v_{\rm w}$ are characteristic flow times for the wind and shock. These expressions for x_1 and x_2 are linear with time and therefore assume that both the wind and shock are moving at constant speed over the region being considered. In this case, the separation L between x_1 and x_2 is also linear with time, and so we can invert Eq. (27) to eliminate t in favor of L, the radial length of the cavity, as the independent variable. The choice to use L makes for easier comparison with the previous case of a forward facing shock.

Fig. 4 shows how the scaled polarisation evolves with the length L. The lower axis is the logarithm of $1+L$. The different curves are for different ratios of $v_{\rm sh}/v_{\rm w} = \tau_{\rm w}/\tau_{\rm sh}$ as indicated. As in Fig. 3, the vertical axis is $p_{\rm shock}$ normalized by the factor $\mu_1(1+\mu_1)$ that accounts for the angular extent of the cone. Substantial values of $p_{\rm shock}$ require fairly low values of $v_{\rm sh}/v_{\rm w} \lesssim 0.5$. This clearly must be the case, for if $v_{\rm sh}/v_{\rm w}$ is near unity, the shock travels outward only slightly slower than the wind so that redistribution occurs over a relatively small volume (i.e., the radial width is small compared to R_*) resulting in little change of polarisation, as is seen for the case $v_{\rm sh}/v_{\rm w} = 0.9$. Only when the wind is speeding away from a much slower shock will the redistribution volume be relatively large. In such cases $p_{\rm shock}$ can become as large as about 0.35 and as small as -0.40 for $v_{\rm sh}/v_{\rm w}$ tending toward zero. In all cases the value of $p_{\rm shock}$ (a) can become zero, (b) is initially positive and then becoming negative, essentially opposite to the trend for a forward facing shock, and (c) shows a maximum for $L \lesssim 0.4$ and minimum at occuring at greater L for smaller ratios of $v_{\rm sh}/v_{\rm w}$.

3.3. Collapse of an equatorial wedge sector to a disk

Another possible source of polarimetric variation could be changes in the oblateness factor of an equatorial wind density enhancement region. For example, using a wedge shaped envelope to approximate a Wind Compressed Zone structure that has been used to describe the axisymmetric density structure of a rotating wind (Ignace et al. 1996), the opening angle of the wedge could evolve with time. Ways for effecting such an evolution arise from variation in the stellar rotation speed $v_{\rm rot}$, the wind acceleration to terminal speed $dv_{\rm r}/dr$, or the terminal speed itself v_∞. For a single star, the first of these (stellar rotation) will change on evolutionary time scales but not over the much shorter wind flush time. Mechanisms leading to for example stellar variability, such as pulsation, could possibly produce changes in the wind acceleration and terminal speed. However such changes might occur, the resulting modification in the polarisation can be described with our theory.

For a fixed interval of radius (x_1, x_2), a variation in the scaled polarisation results from changing the opening angle of the wedge from μ_2 to μ_2', giving

$$p = (\mu_2^2 - \mu_2'^2)\, f(x_1, x_2). \quad (28)$$

Here the change in polarisation is positive for a wedge that becomes more compressed, but can be negative if the wedge were made less compressed. The polarisation is increased in the former case and decreased in the latter. Note that for wedges that are already quite flattened or disc-like (i.e., $\mu_2^2 \ll 1$), there will be little further increase of the polarisation resulting from any additional compression, since both μ_2 and μ_2' are tending to zero.

Alternatively, the compression might occur in radius, so that the wedge geometry in the interval of radius (x_1, x_2) collapses to the interval (x_1', x_2') for μ_2 fixed. The resulting scaled polarisation is thus

$$p = (1 - \mu_2^2)\, [f(x_1', x_2') - f(x_1, x_2)]. \quad (29)$$

Note that the radial dependence of this expression is the same as for radial compression of a conical volume in Sect. 3.2. Thus the results of that section apply here, the only difference being in the angular dependence.

4. Discussion

Our analysis was aimed at confirming and quantifying the point made by Brown (1994) that changes in scattering polarisation by redistibution of electrons within an optically thin wind are likely to be small, or even zero, due to cancellation effects, unless the redistribution is on a large scale in angle or radius. Our results show that this is indeed the case. For example Fig. 2 shows that angular AND radial collapse of a conical cap to a point leads to a relative change in polarisation (i.e., $\Delta p/p = \Delta P/P$) as large as 0.5 of the maximum possible from the point alone (i.e., in a spherical background wind with no cavity) only over a fairly narrow range of parameters. Over fairly substantial ranges, the relative changes are at only the 0–0.2 level. Figs. 3 and 4 show that for a radial compression event (e.g., produced by a radiatively driven shock), optimised parameters lead to a fractional variation in polarisation of only 0.1 (forward facing shock) to 0.35 (rearward facing shock) of that from a conical plume containing the same material.

What this means is that much care is required in claiming that an inhomogeneous wind model predicts the variable polarisation which is observed. Many inhomogeneities developing within a wind will result in wholly undetectable polarisation changes. On the other hand, the fact that polarisation variations *are* observed therefore strongly favours models which result in either very large scale redistribution of wind material (with this occuring rapidly enough so that the material remains close enough to the star to scatter significant light), or models where (possibly more localised) dense blobs emerge from the photosphere as genuine local mass loss enhancements. In calculating the polarisation from any model it is very important to consider the entire wind, including any cavities left by redistribution as these often dominate the nett polarisation.

We emphasise that all our discussion is based on single scattering which will not apply to very dense structures. However, multiple scattering will reduce the polarisation contribution most from the densest regions (i.e., from blobs). This can reduce the cancellation effects we have been discussing and so increase the nett polarisation but with the polarisation dominated by the tenuous cavity contribution rather than by the dense blobs as one might have first expected. For intermediate blob optical depths the outcome should really be computed by formal radiative transfer (e.g., using Monte Carlo techniques as in Code & Whitney 1995).

Acknowledgements. The authors acknowledge support for this work from PPARC Research and Visiting Fellowship Grants and from NSF Grant AST-9417186.

References

Brown J.C., 1994, Ap&SS 221, 357
Brown J.C., McLean I.S., 1977, A&A 57, 141
Brown J.C., McLean I.S., Emslie A.G., 1978, A&A 68, 415
Brown J.C., Carlaw V.A., Cassinelli J.P., 1989, ApJ 344, 341
Brown J.C., Richardson L.L., Antokhin I., et al., 1995, A&A 295, 725
Cassinelli J.P., Swank J.H., 1983, ApJ 271, 681
Cassinelli J.P., Nordsieck K.H., Murison M.A., 1987, ApJ 317, 290
Code A.D., Whitney B.A., 1995, ApJ 441, 400
Daniel J.Y., 1980, A&A 86, 198
Feldmeier A., Puls J., Pauldrach A.W.A., 1997, A&A 322, 878
Gathier R., Lamers H.J.G.L.M., Snow T.P., 1981, ApJ 247, 173
Gayley K.G., Owocki S.P., 1995, ApJ 446, 801
Hundhausen A.J., 1985, In: Stone R.G., Tsurutani T. (eds.) Collisionless Shocks in the Heliosphere: A Tutorial Review. Amer. Geophys. Union, Washington D.C., p. 37
Ignace R., Cassinelli J.P., Bjorkman J.E., 1996, ApJ 459, 671
Kaper L., Henrichs H.F., Nichols J.S., Telting J.H., 1999, A&A 344, 231
Kudritzki R.P., Palsa R., Feldmeier A., Puls J., Pauldrach A.W.A., 1996, In: Zimmermann H.U., Trümper J., Yorke H. (eds.) Röntgenstrahlung from the Universe. MPE Report 263, p. 9
Lamers H.J.G.L.M., Gathier R., Snow T.P., 1982, ApJ 258, 186
Lamers H.J.G.L.M., Cassinelli J.P., 1999, Introduction to Stellar Winds. Cambridge University Press
Langer N., 1998, A&A 329, 551
Li Q., Brown J.C., Ignace R., Cassinelli J.F., Oskinova L., 2000, A&A, in press
Lucy L.B., 1982, ApJ 255, 286
MacFarlane J.J., Cassinelli J.P., 1989, ApJ 347, 1090
Massa D., Fullerton A.W., Nichols J.S., et al., 1995, ApJ 452, L53

Moffat A.F.J., Lepine S., Henriksen R.N., Robert C., 1994, Ap&SS 216, 55
Owocki S.P., Rybicki G.B., 1984, ApJ 284, 337
Richardson L.L., Brown J.C., Simmons J.F.L., 1996, A&A 306, 519
Robert C., 1994, Ap&SS 221, 137
van Vleck J.H., 1925, Proc. Nat. Acad. Sci. 11, 612